

HiTeC: Hierarchical Contrastive Learning on Text-Attributed Hypergraph with Semantic-Aware Augmentation

Mengting Pan¹, Fan Li¹, Xiaoyang Wang¹, Wenjie Zhang¹, Xuemin Lin²

¹University of New South Wales, Sydney, Australia

²Shanghai Jiao Tong University, Shanghai, China

{mengting.pan, fan.li8, xiaoyang.wang1, wenjie.zhang}@unsw.edu.au, xuemin.lin@sjtu.edu.cn

Abstract

Contrastive learning (CL) has become a dominant paradigm for self-supervised hypergraph learning, enabling effective training without costly labels. However, node entities in real-world hypergraphs are often associated with rich textual information, which is overlooked in prior works. Directly applying existing CL-based methods to such text-attributed hypergraphs (TAHGs) leads to three key limitations: (1) The common use of graph-agnostic text encoders overlooks the correlations between textual content and hypergraph topology, resulting in suboptimal representations. (2) Their reliance on random data augmentations introduces noise and weakens the contrastive objective. (3) The primary focus on node- and hyperedge-level contrastive signals limits the ability to capture long-range dependencies, which is essential for expressive representation learning. Although HyperBERT pioneers CL on TAHGs, its co-training paradigm suffers from poor scalability. To fill the research gap, we introduce HiTeC, a two-stage hierarchical contrastive learning framework with semantic-aware augmentation for scalable and effective self-supervised learning on TAHGs. In the first stage, we pre-train the text encoder with a structure-aware contrastive objective to overcome the graph-agnostic nature of conventional methods. In the second stage, we introduce two semantic-aware augmentation strategies, including prompt-enhanced text augmentation and semantic-aware hyperedge drop, to facilitate informative view generation. Furthermore, we propose a multi-scale contrastive loss that extends existing objectives with an s -walk-based subgraph-level contrast to better capture long-range dependencies. By decoupling text encoder pretraining from hypergraph contrastive learning, this two-stage design enhances scalability without compromising representation quality. Extensive experiments on six real-world datasets validate the effectiveness of our proposed method.

1 Introduction

Hypergraphs extend traditional graphs by allowing each hyperedge to connect multiple nodes, offering a natural way to model multi-way relationships. Such higher-order structures are prevalent in complex real-world systems, e.g., cortical co-activation in brains (Yu et al. 2011), user-item interactions in e-commerce platforms (Xia, Huang, and Zhang 2022), and multi-author collaborations in academic networks (Kim et al. 2023). In these scenarios, nodes are often associated with rich textual attributes (e.g., product reviews in user-item networks and paper abstracts in co-authorship

networks), which provide essential semantic information for downstream applications. While Hypergraph Neural Networks (HNNs) have emerged as a powerful paradigm for hypergraph mining (Chien et al. 2022b; Kim et al. 2024b), effectively capturing high-order structural dependencies, they primarily rely on numerical features and task-specific labels. This reliance limits their effectiveness in real-world applications, where labeled data is scarce and node attributes are predominantly textual. Therefore, underscoring the necessity and significance of self-supervised learning (SSL) on Text-Attributed Hypergraphs (TAHGs).

Recent advances in hypergraph self-supervised learning (HSSL) have primarily focused on contrastive learning paradigms, which aim to maximize the agreement between two augmented views derived from the original hypergraph. HyperGCL (Wei et al. 2022) pioneers this line of work by employing a learnable augmentation strategy. TriCL (Lee and Shin 2023) introduces tri-directional contrastive objectives that model node-, hyperedge-, and membership-level relations in hypergraphs. SE-HSSL (Li et al. 2024) extends this framework by re-designing a hierarchical membership-level objective, achieving state-of-the-art (SOTA) performance. Beyond contrastive methods, generative approaches have also gained initial attention. HypeBoy (Kim et al. 2024a) proposes a hyperedge-filling pretext task to learn expressive hypergraph representations.

Despite recent progress, current HSSL approaches still encounter significant limitations when adopted to hypergraphs with textual attributes: (1) They typically use shallow encoders (e.g., Bag-of-Words (Zhang, Jin, and Zhou 2010) and Skip-Gram (Mikolov et al. 2013)) or pre-trained language models (e.g., BERT (Devlin et al. 2019)) to convert raw text into numerical features, ignoring hypergraph structure. This graph-agnostic design overlooks the correlation between text and higher-order topology, leading to suboptimal representations (Chien et al. 2022a). (2) Current hypergraph contrastive learning (HCL) methods often apply random augmentations to features and structure, such as randomly masking text or hyperlinks. Such perturbations can distort textual meaning and disrupt the alignment between structure and semantic content, thereby introducing noise into the contrastive objective (Fang et al. 2024). (3) Existing HCL methods primarily focus on node- and hyperedge-level signals, while overlooking long-range dependencies

and complex topological contexts, which are essential for learning expressive representations (Zhang et al. 2024).

HyperBERT (Bazaga, Lio, and Micklem 2024) takes an early attempt at SSL on TAHGs by jointly encoding textual semantics and hypergraph structure via a Transformer-based architecture. However, its co-training paradigm incurs substantial memory overhead, limiting scalability even on medium-sized hypergraphs (e.g., History and Photo (Yan et al. 2023)), as demonstrated in our experiments. Moreover, it focuses solely on node-level contrastive signals, ignoring multi-scale structural information that has proven beneficial for HSSL (Lee and Shin 2023; Li et al. 2024). Although recent text-attributed graph studies (Chien et al. 2022a; Fang et al. 2024; Zhang et al. 2024) explore joint modeling of text and structure, they overlook high-order relations in hypergraphs, which may limit their applicability to TAHGs.

To address these issues, we propose HiTeC, a hierarchical contrastive learning framework with semantic-aware augmentation for scalable and effective SSL on TAHGs. HiTeC adopts a two-stage design that decouples the pretraining of the text and hypergraph encoders, significantly improving the scalability over joint training paradigms. To overcome the graph-agnostic nature of existing text encoders, we first introduce a structure-aware contrastive objective during text encoder pretraining. Positive and negative text pairs are constructed based on structural proximity, encouraging the encoder to capture correlations between textual content and higher-order topology. Furthermore, to mitigate the noise introduced by random augmentations, we propose two semantic-aware augmentation strategies: a prompt-enhanced text augmentation module, which injects structural context into raw text to generate diverse yet semantically consistent views, and a semantic-aware hyperedge drop mechanism, which discards hyperedges according to their internal semantic cohesion to preserve meaningful relational patterns. Finally, to capture long-range dependencies and multi-scale structural knowledge, we formulate hierarchical contrastive objectives at the node, hyperedge, and subgraph levels. Specifically, our subgraph contrastive objective leverages an s -walk-based sampling strategy to extract structurally informative subgraphs, facilitating representation learning over broader contexts. Our main contributions are summarized as follows:

- We propose HiTeC, a scalable and effective two-stage contrastive learning framework for TAHGs, addressing key limitations of existing HSSL methods in modeling complex structural dependencies and rich textual content.
- We introduce a structure-aware contrastive objective to pre-train the text encoder, enabling integration of textual content with hypergraph structure, and overcoming the graph-agnostic nature of existing text encoders.
- We enhance the hypergraph encoder with semantic-aware augmentations and hierarchical contrastive objectives. Specifically, a prompt-enhanced text augmentation and semantic-aware hyperedge drop strategies are designed to reduce perturbation noise. And a novel s -walk-based subgraph-level signal is employed to capture long-range structural dependencies.

- We conduct a comprehensive evaluation of HiTeC on six real-world datasets. The experimental results demonstrate its superiority over strong baselines across various benchmark downstream tasks.

2 Preliminary

Notations. We define a text-attributed hypergraph (TAHG) as $\mathcal{H} = \{\mathcal{V}, \mathcal{E}, \mathcal{T}\}$, where $\mathcal{V} = \{v_i\}_{i=1}^{|\mathcal{V}|}$ denotes the set of nodes, and $\mathcal{E} = \{e_j\}_{j=1}^{|\mathcal{E}|}$ denotes the set of hyperedges, with each hyperedge $e \in \mathcal{E}$ is a non-empty subset of nodes, and $|e|$ is the size of e . Each node v_i is associated with a textual sequence $t_i \in \mathcal{T}$, and \mathcal{T} represents the set of all text attributes. Each hyperedge e_j is associated with a positive scalar weight w_j , and all weights formulate a diagonal matrix $\mathbf{W} \in \mathbb{R}^{|\mathcal{E}| \times |\mathcal{E}|}$. The hypergraph structure can be modeled as an incidence matrix $\mathbf{H} \in \{0, 1\}^{|\mathcal{V}| \times |\mathcal{E}|}$, where $h_{ij} = 1$ if node v_i belongs to hyperedge e_j , and $h_{ij} = 0$ otherwise. We define the node degree matrix $\mathbf{D}_v \in \mathbb{R}^{|\mathcal{V}| \times |\mathcal{V}|}$, where each entry is $d(v_i) = \sum_{e_j \in \mathcal{E}} w_j \cdot h_{ij}$. Similarly, the hyperedge degree matrix is defined as $\mathbf{D}_e \in \mathbb{R}^{|\mathcal{E}| \times |\mathcal{E}|}$, where each element $\delta(e_j) = \sum_{v_i \in e_j} h_{ij}$ represents the number of nodes connected by the hyperedge e_j .

Hypergraph neural networks. Hypergraph neural networks (HNNs) have emerged as effective models for representation learning on hypergraphs (Feng et al. 2019; Bai, Zhang, and Torr 2021; Chien et al. 2022b). Most HNNs adopt a two-stage message passing mechanism that alternates between node-to-hyperedge and hyperedge-to-node aggregation. At each layer l , the embedding of a hyperedge is updated based on its incident nodes, while a node embedding is updated via its associated hyperedges:

$$\begin{aligned} z_{e_j}^{(l)} &= f_{\mathcal{V} \rightarrow \mathcal{E}}^{(l)} \left(z_{e_j}^{(l-1)}, \{z_{v_k}^{(l-1)} \mid v_k \in e_j\} \right), \\ z_{v_i}^{(l)} &= f_{\mathcal{E} \rightarrow \mathcal{V}}^{(l)} \left(z_{v_i}^{(l-1)}, \{z_{e_k}^{(l)} \mid v_i \in e_k\} \right), \end{aligned} \quad (1)$$

where $z_{e_j}^{(l)}$ and $z_{v_i}^{(l)}$ denote the embeddings of hyperedge e_j and node v_i at layer l , respectively. The functions $f_{\mathcal{V} \rightarrow \mathcal{E}}^{(l)}$ and $f_{\mathcal{E} \rightarrow \mathcal{V}}^{(l)}$ are permutation-invariant aggregation functions that propagate messages between nodes and hyperedges. This iterative process allows the model to capture complex high-order relations in the hypergraph structure.

Problem statement. Given a TAHG $\mathcal{H} = \{\mathcal{V}, \mathcal{E}, \mathcal{T}\}$, the objective is to learn an optimal function $\Psi : \mathcal{H} \rightarrow (\mathbf{Z}_{\mathcal{V}}, \mathbf{Z}_{\mathcal{E}})$ in an unsupervised manner that maps the hypergraph to low-dimensional embeddings of nodes and hyperedges. These representations may then be applied to downstream tasks such as node classification and hyperedge prediction.

3 Methodology

3.1 Overview

As illustrated in Figure 1, we present HiTeC, a contrastive learning framework tailored for TAHGs. In the first stage, we pre-train the text encoder f_{θ} with a structure-aware contrastive objective, allowing it to capture topological knowledge and achieve more expressive text representations than

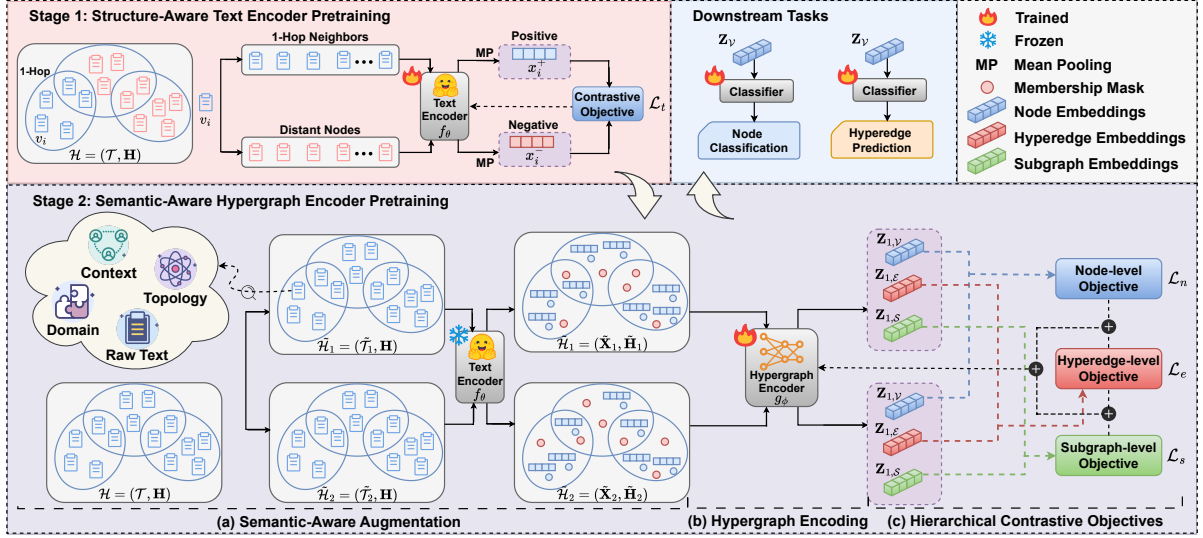


Figure 1: The overall framework of HiTeC.

graph-agnostic encoders. In the second stage, we pre-train a hypergraph encoder g_ϕ with f_θ frozen. To fully exploit the rich semantic context of nodes, we introduce two semantic-aware augmentation strategies on both text- and structure-level, enhancing view diversity while preserving semantic coherence. Furthermore, we design a hierarchical contrastive objective across node, hyperedge, and subgraph levels. Specifically, the subgraph-level objective, enabled by s -walk sampling, captures long-range dependencies. By decoupling the training of two encoders, HiTeC achieves better scalability and performance in integrating textual content and high-order structures.

3.2 Structure-aware Text Encoder Pretraining

Text encoder. Our text encoder f_θ is built upon a pre-trained language model (PLM) (e.g., BERT (Devlin et al. 2019)) with a lightweight projection layer. To enable efficient training, we apply the parameter-efficient approach, LoRA (Hu et al. 2022). Given a node $v_i \in \mathcal{V}$ with textual attribute t_i , the textual representation is formulated as:

$$x_i = f_\theta(t_i), \quad (2)$$

where $x_i \in \mathbb{R}^d$ denotes the embedding corresponding to the [CLS] token in the output sequence.

Structure-aware contrastive objective. In real-world hypergraphs, nodes are often semantically closer to their local neighbors than to distant ones. For example, in co-citation hypergraphs, papers within the same hyperedge tend to be more topically related. To encode these structural priors, we pre-train f_θ by contrasting local and distant semantic contexts. Specifically, for each node $v_i \in \mathcal{V}$, we treat its 1-hop neighbors $N_{v_i}^{(1)}$ as positives, and nodes beyond 1-hop distance $\mathcal{V} \setminus N_{v_i}^{(1)}$ as negatives. As shown in Figure 1, 1-hop neighbors are defined as nodes belong to the same hyperedges that contain v_i . Contrastive pairs are constructed by

mean pooling embeddings from each set:

$$\begin{aligned} x_i^+ &= \frac{1}{|N_{v_i}^{(1)}|} \sum_{v_j \in N_{v_i}^{(1)}} f_\theta(t_j), \\ x_i^- &= \frac{1}{|\mathcal{V} \setminus N_{v_i}^{(1)}|} \sum_{v_j \in \mathcal{V} \setminus N_{v_i}^{(1)}} f_\theta(t_j), \end{aligned} \quad (3)$$

where $x_i^+ \in \mathbb{R}^d$ and $x_i^- \in \mathbb{R}^d$ denote the aggregated representations of the positive and negative samples, respectively.

A triplet margin loss (Schroff, Kalenichenko, and Philbin 2015) is adopted to guide f_θ in distinguishing positive sample x_i^+ from negative sample x_i^- . For each anchor x_i , the loss of the text encoder is defined as:

$$\ell_t(x_i, x_i^+, x_i^-) = \max\{\cos(x_i, x_i^+) - \cos(x_i, x_i^-) + m\}, \quad (4)$$

where $\cos(\cdot)$ denotes cosine similarity, and m is the margin hyperparameter. The overall structure-aware objective is averaged across all nodes:

$$\mathcal{L}_t = \frac{1}{|\mathcal{V}|} \sum_{v_i \in \mathcal{V}} \ell_t(x_i, x_i^+, x_i^-), \quad (5)$$

This process allows f_θ to incorporate structural signals into textual representations.

3.3 Semantic-aware Hypergraph Encoder Pretraining

Existing HCL methods often overlook node textual semantics and rely on random augmentation strategies, resulting in suboptimal performance (Fang et al. 2024; Wu et al. 2024). Moreover, they struggle to model long-range dependencies, limiting broader contextual understanding (Zhang et al. 2024; Wu et al. 2024). To tackle these issues, we propose a semantic-aware contrastive learning strategy to pre-train g_ϕ . As shown in Figure 1, this stage comprises three

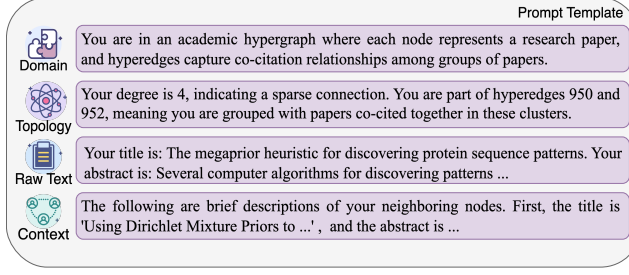


Figure 2: An example of the prompt template on Cora.

components: semantic-aware augmentation, hypergraph encoding, and hierarchical contrastive objectives.

Semantic-aware augmentation. To mitigate the noise from random perturbations, we introduce two novel augmentation techniques: prompt-enhanced text augmentation, which generates diverse yet semantically consistent textual views, and semantic-aware hyperedge drop, which ensures structural perturbations remain aligned with the semantics.

Prompt-enhanced text augmentation. As feature-level perturbations can easily distort semantic meaning, we instead focus on augmenting the raw text using a prompt-enhanced strategy. For each node text t_i , we construct an augmented view $\tilde{t}_{1,i} = \text{Prompt}(t_i, \mathcal{H})$, while retaining the original text as $\tilde{t}_{2,i} = t_i$. As shown in Figure 2, the prompt template integrates the original text with domain knowledge, global topology, and neighbor context, concatenated into a single sequence. Each component adds a distinct perspective: domain knowledge offers semantic background, global topology introduces structural awareness, and neighbor context provides complementary local semantics. This simple yet effective strategy generates semantically consistent but contextually diverse text variants, with a shared f_θ that maps them to a unified space, denoted as $\tilde{\mathbf{X}}_1$ and $\tilde{\mathbf{X}}_2$, respectively.

Semantic-aware hyperedge drop. Effective structure augmentation should consider both textual semantics and the original topology. To achieve that, we define a semantic cohesiveness score that reflects both the structural grouping of nodes and their semantic similarity. This score is then used to guide the drop probability of each node–hyperedge incidence: connections within more cohesive hyperedges are more likely to be preserved. In this way, our strategy encourages the retention of structurally and semantically aligned patterns, while selectively pruning noisy or weakly related hyperlinks. We formally define the it as follows.

Definition 1 (semantic cohesiveness score). Given a TAHG $\mathcal{H}(\mathcal{V}, \mathcal{E}, \mathbf{X})$, the semantic cohesiveness score of a hyperedge $e \in \mathcal{E}$ is defined as the average pairwise cosine similarity among its member nodes. Let $\mathbf{X}_e \in \mathbb{R}^{|e| \times d}$ denote the normalized feature matrix for nodes in e . The semantic cohesiveness score $s(e)$ is then computed as:

$$s(e) = \frac{1}{\binom{|e|}{2}} \sum_{i=1}^{|e|} \sum_{j=i+1}^{|e|} S_e(i, j), \quad S_e = \mathbf{X}_e \mathbf{X}_e^\top,$$

where $S_e(i, j)$ denotes the similarity between the i -th and j -th node in hyperedge e .

The drop probability of each node-hyperedge incidence (v_i, e_j) where $v_i \in e_j$ is then guided by $s(e_j)$:

$$p_{\text{drop}}(v_i, e_j) = 1 - \sigma \left(\frac{s(e_j) - 0.5}{\tau_{\text{drop}}} \right), \quad (6)$$

where $\sigma(\cdot)$ is the sigmoid function and τ_{drop} is a temperature hyperparameter. Higher cohesiveness scores lead to lower drop probabilities. In implementation, we construct a binary masking matrix $\mathbf{M} \in \{0, 1\}^{|\mathcal{V}| \times |\mathcal{E}|}$, where each entry $m_{ij} \sim \mathcal{B}(1 - p_{\text{drop}}(v_i, e_j))$ is sampled from a Bernoulli distribution. The perturbed incidence matrix $\tilde{\mathbf{H}}$ is represented as:

$$\tilde{\mathbf{H}} = \mathbf{M} \odot \mathbf{H}, \quad (7)$$

where \odot denotes element-wise multiplication. We apply this semantic-aware hyperedge drop mechanism to both views, yielding two augmented hypergraphs: $\tilde{\mathcal{H}}_1 = (\tilde{\mathbf{X}}_1, \tilde{\mathbf{H}}_1)$ and $\tilde{\mathcal{H}}_2 = (\tilde{\mathbf{X}}_2, \tilde{\mathbf{H}}_2)$. This procedure complements text-level augmentation by introducing structural diversity while retaining semantic consistency, enabling the hypergraph encoder to learn more robust node representations.

Hypergraph encoder. We take the HGNN (Feng et al. 2019) with the element-wise mean pooling layer as our hypergraph encoder. At the l -th layer, the hyperedge representation $\mathbf{Z}_\mathcal{E}^{(l)} \in \mathbb{R}^{|\mathcal{E}| \times d}$ and the node representation $\mathbf{Z}_\mathcal{V}^{(l)} \in \mathbb{R}^{|\mathcal{V}| \times d}$ are updated as:

$$\begin{aligned} \mathbf{Z}_\mathcal{E}^{(l)} &= \rho \left(\mathbf{D}_e^{-1} \mathbf{H}^\top \mathbf{Z}_\mathcal{V}^{(l-1)} \Theta_\mathcal{E}^{(l)} + \mathbf{b}_e^{(l)} \right), \\ \mathbf{Z}_\mathcal{V}^{(l)} &= \rho \left(\mathbf{D}_v^{-1} \mathbf{H} \mathbf{W} \mathbf{Z}_\mathcal{E}^{(l)} \Theta_\mathcal{V}^{(l)} + \mathbf{b}_v^{(l)} \right), \end{aligned} \quad (8)$$

where $\rho(\cdot)$ is the PReLU activation function, $\Theta_\mathcal{E}^{(l)}$ and $\Theta_\mathcal{V}^{(l)}$ are trainable weight matrices, and $\mathbf{b}_e^{(l)}$ and $\mathbf{b}_v^{(l)}$ are corresponding bias terms. \mathbf{W} is initialized as an identity matrix, which means equal weights for all hyperedges.

Hierarchical contrastive objectives. Prior works (Lee and Shin 2023; Li et al. 2024) have demonstrated that multi-scale contrastive objectives are beneficial for HSSL. To better capture structural semantics at different granularities, we adopt a hierarchical contrastive learning objective spanning node, hyperedge, and subgraph levels. In particular, the novel subgraph-level objective, based on s -walk sampling, enables the model to capture long-range dependencies beyond local structure. All objectives are optimized with InfoNCE loss (Oord, Li, and Vinyals 2018).

Node-level objective. We first model the correlation of nodes across two augmented views. Given a node $v_i \in \mathcal{V}$, let \mathbf{z}_{1,v_i} and \mathbf{z}_{2,v_i} denote its node embeddings derived from two augmented hypergraphs. By fixing \mathbf{z}_{1,v_i} as anchor, we treat $(\mathbf{z}_{1,v_i}, \mathbf{z}_{2,v_i})$ as a positive pair, and all \mathbf{z}_{2,v_k} for $k \neq i$ as negative samples. The loss of anchor \mathbf{z}_{1,v_i} is:

$$\ell_n(\mathbf{z}_{1,v_i}, \mathbf{z}_{2,v_i}) = -\log \frac{e^{\cos(\mathbf{z}_{1,v_i}, \mathbf{z}_{2,v_i})/\tau_n}}{\sum_{k=1}^{|\mathcal{V}|} e^{\cos(\mathbf{z}_{1,v_i}, \mathbf{z}_{2,v_k})/\tau_n}}, \quad (9)$$

where τ_n is the temperature coefficient. In practice, we symmetrize the loss by using the second view’s embedding as

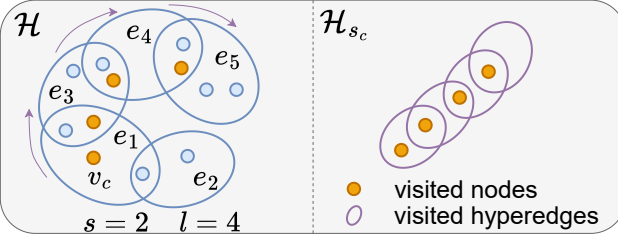


Figure 3: An example of the s -walk-based subgraph sampling process. For center node v_c , we perform s -walk with $s = 2$ and $l = 4$ on \mathcal{H} . The hyperedge sequences visited are $[e_1, e_3, e_4, e_5]$. The sampled subgraph is denoted as \mathcal{H}_{s_c} .

the anchor and obtain the final node-level contrastive loss:

$$\mathcal{L}_n = \frac{1}{2|\mathcal{V}|} \sum_{i=1}^{|\mathcal{V}|} [\ell_n(\mathbf{z}_{1,v_i}, \mathbf{z}_{2,v_i}) + \ell_n(\mathbf{z}_{2,v_i}, \mathbf{z}_{1,v_i})]. \quad (10)$$

Hyperedge-level objective. To consider group-level knowledge, we integrate hyperedge-level contrastive signal during optimization. Given a hyperedge $e_j \in \mathcal{E}$, let \mathbf{z}_{1,e_j} and \mathbf{z}_{2,e_j} be its hyperedge representations from the two augmented views. Similar to the node-level objective, the contrastive loss with \mathbf{z}_{1,e_j} as anchor is formulated as:

$$\ell_e(\mathbf{z}_{1,e_j}, \mathbf{z}_{2,e_j}) = -\log \frac{e^{\cos(\mathbf{z}_{1,e_j}, \mathbf{z}_{2,e_j})/\tau_e}}{\sum_{k=1}^{|\mathcal{E}|} e^{\cos(\mathbf{z}_{1,e_j}, \mathbf{z}_{2,e_k})/\tau_e}}, \quad (11)$$

where τ_e is the temperature coefficient. Symmetrizing the loss, the final hyperedge-level objective can be written as:

$$\mathcal{L}_e = \frac{1}{2|\mathcal{E}|} \sum_{j=1}^{|\mathcal{E}|} [\ell_e(\mathbf{z}_{1,e_j}, \mathbf{z}_{2,e_j}) + \ell_e(\mathbf{z}_{2,e_j}, \mathbf{z}_{1,e_j})]. \quad (12)$$

Subgraph-level objective. While node- and hyperedge-level objectives capture local semantic and structural signals, they may fail to model long-range dependencies in hypergraphs. To bridge this gap, we further introduce a subgraph-level objective by constructing broader structural signals through a novel s -walk-based sampling strategy. Unlike random walk, s -walk is a high-order sequence in hypergraphs, where s measures the overlap strength between hyperedges, enabling the extraction of cohesive and semantically meaningful substructures unique to hypergraphs (Aksoy et al. 2020; Preti, De Francisci Morales, and Bonchi 2024). We next define s -walk and detail our subgraph sampling method.

Definition 2 (s -walk). Given $s \in \mathbb{N}^+$, an s -walk of length l is a sequence of hyperedges $[e_1, \dots, e_l]$ such that each consecutive pair of hyperedges shares at least s nodes, i.e., $|e_j \cap e_{j+1}| \geq s$ for all $j \in [1, l-1]$.

As illustrated in Figure 3, we construct an s -walk-based subgraph $\mathcal{H}_{s_c} = \{\mathcal{V}_{s_c}, \mathcal{E}_{s_c}\}$ by first selecting a starting hyperedge e_1 that contains the center node v_c , and then performing an s -walk of length l . We randomly sample one node from each visited hyperedge. The sampled subgraph includes all visited hyperedges and their associated nodes:

Dataset	$ \mathcal{V} $	$ \mathcal{E} $	Avg. $ e $	# Avg. tokens	# Class
Citeseer	1,778	2,118	2	198	6
Cora	2,708	1,579	3	189	7
History	41,551	169,454	9	300	12
Photo	48,362	212,247	11	189	12
Computers	87,229	277,539	9	115	10
Fitness	173,055	1,468,229	11	28	13

Table 1: Statistics of datasets.

$\mathcal{E}_{s_c} = \{e_j\}_{j=1}^l$, $\mathcal{V}_{s_c} = \bigcup_{j=1}^l e_j$. Each subgraph \mathcal{H}_{s_c} can be encoded by the shared hypergraph encoder $g_\phi(\cdot)$, and its representation is obtained via mean pooling P_{mean} over the node embeddings:

$$\mathbf{z}_{s_c} = P_{\text{mean}}(g_\phi(\mathcal{H}_{s_c})). \quad (13)$$

However, constructing and encoding subgraphs for all nodes incurs a high computational cost. To mitigate this, we follow prior findings suggesting that high-degree nodes tend to carry richer contextual information (Fang et al. 2025). Specifically, we select a subset of representative nodes $\mathcal{V}_r \subseteq \mathcal{V}$ by ranking node degrees and retaining the top $r\%$. As validated in our experiments, this strategy maintains competitive performance even with a significantly reduced number of subgraphs. For each anchor node $v_m \in \mathcal{V}_r$, we obtain subgraph representations \mathbf{z}_{1,s_m} and \mathbf{z}_{2,s_m} from two augmented views. Similar to the former contrastive signals, the subgraph-level loss with anchor \mathbf{z}_{1,s_m} is defined as:

$$\ell_s(\mathbf{z}_{1,s_m}, \mathbf{z}_{2,s_m}) = -\log \frac{e^{\cos(\mathbf{z}_{1,s_m}, \mathbf{z}_{2,s_m})/\tau_s}}{\sum_{k=1}^{|\mathcal{V}_r|} e^{\cos(\mathbf{z}_{1,s_m}, \mathbf{z}_{2,s_k})/\tau_s}}, \quad (14)$$

where τ_s is a temperature coefficient. And the final symmetric loss across all anchors is:

$$\mathcal{L}_s = \frac{1}{2|\mathcal{V}_r|} \sum_{m=1}^{|\mathcal{V}_r|} [\ell_s(\mathbf{z}_{1,s_m}, \mathbf{z}_{2,s_m}) + \ell_s(\mathbf{z}_{2,s_m}, \mathbf{z}_{1,s_m})]. \quad (15)$$

Overall objective. Finally, by integrating Eq. (10), (12), and (15), our proposed contrastive loss is formulated as:

$$\mathcal{L} = \mathcal{L}_n + \lambda_e \mathcal{L}_e + \lambda_s \mathcal{L}_s, \quad (16)$$

where λ_e and λ_s are balancing weights. This hierarchical contrastive framework enables the model to capture patterns at multiple granularities, generating more robust and discriminative node representations.

4 Experiments

4.1 Experimental Setup

Datasets. Since there are no publicly available TAHG datasets, we introduce six new text-attributed hypergraph datasets using a max clique-based hypergraph reconstruction method (Bron and Kerbosch 1973; Wang and Kleinberg 2024). These include two co-citation hypergraphs: Citeseer (Giles, Bollacker, and Lawrence 1998) and Cora (Sen et al. 2008), and four co-purchasing networks: History, Photo, Computers, and Fitness (Yan et al. 2023). Detailed

Method	Citeseer	Cora	History	Photo	Computers	Fitness
Graph SSL	GraphCL + SE	59.63 ± 1.58	56.69 ± 1.99	62.86 ± 0.22	42.61 ± 0.21	34.45 ± 0.38
	GraphCL + GIANT	57.58 ± 1.90	55.64 ± 1.50	62.08 ± 0.24	42.74 ± 0.22	34.65 ± 0.23
	BGRL + SE	60.81 ± 1.45	59.72 ± 1.32	65.74 ± 0.30	44.60 ± 0.30	39.40 ± 0.46
	BGRL + GIANT	58.68 ± 1.92	57.44 ± 1.39	63.99 ± 0.35	43.65 ± 0.25	37.00 ± 0.37
	GraphMAE + SE	46.42 ± 2.75	50.33 ± 0.47	52.90 ± 9.01	41.52 ± 0.08	25.61 ± 0.11
	GraphMAE + GIANT	50.11 ± 1.74	53.59 ± 1.07	56.20 ± 0.12	41.54 ± 0.06	25.57 ± 0.12
HSSL	TriCL + SE	60.78 ± 1.00	58.79 ± 1.30	69.28 ± 0.32	47.11 ± 0.44	43.43 ± 0.66
	TriCL + BERT	64.50 ± 1.08	62.67 ± 1.13	75.01 ± 0.22	51.25 ± 0.62	46.60 ± 0.90
	TriCL + RoBERTa	64.48 ± 0.95	60.74 ± 1.01	70.62 ± 0.81	48.42 ± 0.67	43.82 ± 1.11
	SE-HSSL + SE	57.04 ± 3.31	59.87 ± 1.83	68.59 ± 0.74	43.75 ± 2.01	36.53 ± 2.32
	SE-HSSL + BERT	65.83 ± 1.21	64.30 ± 0.89	74.88 ± 0.42	51.80 ± 0.63	41.63 ± 2.21
	SE-HSSL + RoBERTa	65.04 ± 1.04	62.76 ± 1.15	72.13 ± 1.07	49.41 ± 2.62	40.86 ± 3.99
	HypeBoy + SE	59.98 ± 2.45	29.87 ± 0.62	OOM	OOM	OOM
	HypeBoy + BERT	61.98 ± 1.70	32.73 ± 1.71	OOM	OOM	OOM
	HypeBoy + RoBERTa	50.41 ± 2.88	30.84 ± 0.95	OOM	OOM	OOM
	VilLain (w/o feat.)	42.22 ± 1.72	53.72 ± 1.00	40.99 ± 3.06	33.94 ± 1.39	20.99 ± 0.91
HiTeC	HyperBERT	30.25 ± 3.04	26.85 ± 0.66	OOM	OOM	OOM
		66.38 ± 1.73	74.07 ± 0.88	79.81 ± 0.16	59.64 ± 0.16	55.81 ± 0.12
						67.18 ± 0.19

Table 2: Node classification accuracy (% mean \pm std) across six datasets. The **best** and second-best results are highlighted in **bold** and underline, respectively. “w/o feat.” means without node features. OOM denotes out-of-memory on a 24GB GPU.

dataset statistics are presented in Table 1, with comprehensive descriptions provided in Appendix A.1.

Baselines. We compare HiTeC with seven strong SSL baselines covering both graph- and hypergraph-based methods. Since these methods cannot handle raw text directly, we extract features using shallow encoders (SE), PLMs (BERT (Devlin et al. 2019), RoBERTa (Liu et al. 2019)), and graph-agnostic encoder (GIANT (Chien et al. 2022a)). Full details are provided in Appendix A.2.

Evaluation protocol. We evaluate our approach on two hypergraph benchmark tasks: node classification and hyperedge prediction. After pretraining with HiTeC, we follow the linear evaluation protocol (Lee and Shin 2023; Li et al. 2024; Kim et al. 2024a), where the learned node embeddings are fixed and used as inputs to downstream classifiers. Full evaluation details are provided in Appendix A.3.

Implementation details. All baselines use official implementations with default settings. For HiTeC, we tune the contrastive loss weights λ_e and λ_s over $\{1, 2, 3, 4\}$. The overlap size s is selected from $\{1, 2, 3, 4, 5, 10\}$, and the sampling ratio $r\%$ from $\{10\%, 20\%, 30\%, 40\%, 50\%\}$. Full implementation details are provided in Appendix A.4.

4.2 Main Results

We evaluate our approach on two hypergraph tasks: node classification and hyperedge prediction (see Appendix B.1).

Node classification evaluation. We first evaluate HiTeC on the node classification task. Table 2 presents the results, revealing two key observations: (1) Graph-based SSL methods perform consistently worse than HSSL methods. This is primarily due to the loss of high-order relations caused by clique expansion. Even GIANT, which incorporates textual and structural signals, remains insufficient for modeling high-order structures. These results highlight the necessity of developing SSL methods tailored for TAHG. (2) HiTeC achieves the best overall performance with strong scalabil-

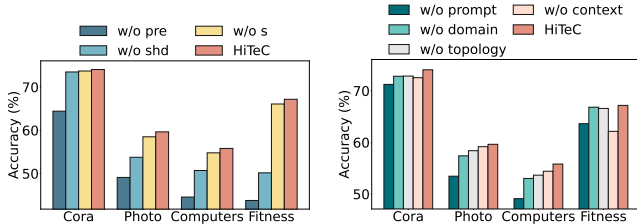
ity. VilLain performs poorly due to its neglect of textual information, highlighting the critical role of node semantics. TriCL and SE-HSSL also underperform, mainly because of inadequate textual feature extraction and limited modeling of long-range dependencies. While both HyperBERT and HiTeC integrate textual semantics with high-order structure, HyperBERT fails to fully exploit semantic-structural signals and cannot scale to even medium-sized hypergraphs (e.g., History, Photo) due to its joint modeling scheme. In contrast, HiTeC consistently outperforms all baselines, surpassing the second-best method by 9.77% and 10.26% on Cora and Fitness, respectively. This is attributed to the semantic-aware augmentations and s -walk-based subgraph contrast, which reduce perturbation noise and enable the model to capture more global dependencies. Furthermore, our two-stage decoupled design brings scalability, with the structure-aware contrastive objective complementing it while preserving high performance.

4.3 Ablation Study

We conduct ablation studies on: (1) key components of HiTeC, (2) prompt template elements, and (3) text encoder backbones (see Appendix B.2).

Impact of components. We first assess the contribution of each component in HiTeC. As shown in Figure 4(a), removing any module results in a performance drop. The most severe drop is caused by “w/o pre”, with 11.25% and 23.41% declines on Computers and Fitness, respectively. This highlights the importance of incorporating topology into the text encoder for learning expressive textual representations. Semantic-aware hyperedge drop is also critical, as its removal (“w/o shd”) leads to a 17.02% drop on Fitness, demonstrating the value of maintaining semantic consistency during structural perturbation.

Impact of prompt. We further analyze the effect of prompt design in Figure 4(b). Overall, our prompt-enhanced aug-



(a) Impact of components.

(b) Impact of prompt.

Figure 4: Ablation study. (a) Impact of components: “w/o pre” removes the structure-aware pre-training of the text encoder; “w/o shd” replaces the semantic-aware hyperedge drop with the random drop; and “w/o s” removes the subgraph-level contrastive objective. (b) Impact of prompt: “w/o prompt” uses original text only; “w/o domain”, “w/o topology”, and “w/o context” remove the corresponding content from the prompt template.

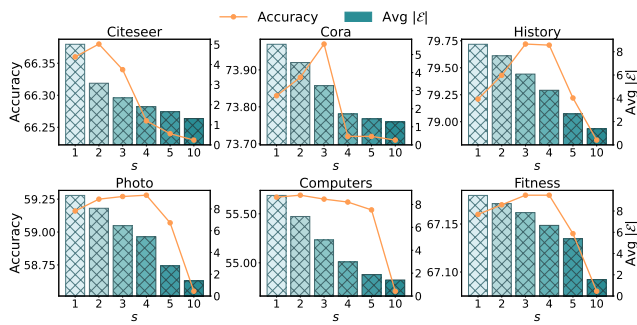


Figure 5: Sensitive analysis of s . The line plot shows model accuracy under different values of s . The bar plot indicates the average number of hyperedges in the sampled subgraph, reflecting its exploration range.

mentation outperforms other variants. “w/o prompt” yields the largest performance drop, confirming the benefits of injecting diverse semantics into text augmentation. Removing individual content, such as context or topology, also leads to noticeable declines, highlighting the importance of incorporating meaningful structural signals into the original text.

4.4 Parameter Sensitivity Analysis

We conduct sensitivity experiments on two key hyperparameters: the overlap size s in the s -walk, and the subgraph sampling ratio r (see Appendix B.3).

Overlap size s . Figure 5 illustrates how model performance varies with different values of s , where model performance first improves and then degrades as s increases. This trend can be attributed to the trade-off between structural coherence and exploration: when the exploration range remains sufficiently broad, a larger s promotes more cohesive subgraphs while preserving essential contextual semantics. However, excessively strict overlap constraints (e.g., $s=10$) limit structural diversity and impair performance. Figure 6 further indicates that increasing s leads to smaller sub-

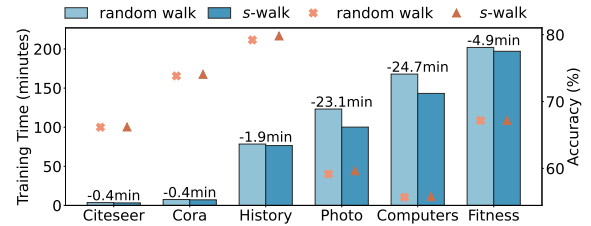


Figure 6: Training time vs. accuracy of random walk and s -walk. Bars indicate training time, markers denote accuracy.

graphs, thereby accelerating training. These results highlight the importance of selecting an appropriate s to balance accuracy and efficiency.

5 Related Work

Our work is closely related to self-supervised learning on hypergraphs and representation learning on text-attributed graphs (see Appendix C.1).

5.1 Self-supervised Learning on Hypergraphs

SSL provides a promising alternative for hypergraph representation learning without expensive labels. Most existing HSSL methods focus on contrastive learning. HyperGCL (Wei et al. 2022) introduces a learnable augmentation strategy, while TriCL (Lee and Shin 2023) and SE-HSSL (Li et al. 2024) design hierarchical objectives across multiple granularities. Beyond contrastive approaches, generative SSL has also emerged, with HypeBoy (Kim et al. 2024a) proposing a hyperedge-filling task. Other efforts address different settings, such as Villain (Lee, Lee, and Shin 2024), which targets feature-absent scenarios. While effective in modeling high-order structure, these methods overlook the rich textual semantics in TAHGs. HyperBERT (Bazaga, Lio, and Micklem 2024) pioneers SSL on TAHGs by jointly encoding textual semantics and hypergraph structure, but it incurs high computational overhead and suffers from poor scalability. To bridge the gap, we explore a scalable and effective contrastive learning framework for TAHGs.

6 Conclusion

We propose HiTeC, a hierarchical contrastive learning framework with semantic-aware enhancement, to address limitations of existing HCL methods in TAHGs. To ensure scalability, HiTeC adopts a two-stage decoupled paradigm. The first stage pre-trains a text encoder with a structure-aware contrastive objective, alleviating the graph-agnostic nature of conventional encoders. In the second stage, two semantic-aware augmentation strategies, including prompt-enhanced text augmentation and semantic-aware hyperedge drop, are designed to generate more informative hypergraph views. Furthermore, we introduce a hierarchical contrastive objective, where a novel s -walk-based subgraph-level contrast captures long-range structural dependencies beyond node and hyperedge scopes. Extensive experiments on six real-world datasets and multiple downstream tasks demonstrate the effectiveness and scalability of HiTeC.

References

Aksoy, S. G.; Joslyn, C.; Marrero, C. O.; Praggastis, B.; and Purvine, E. 2020. Hypernetwork science via high-order hypergraph walks. *EPJ Data Science*, 9(1): 16.

Bai, S.; Zhang, F.; and Torr, P. H. 2021. Hypergraph convolution and hypergraph attention. *Pattern Recognition*, 110: 107637.

Bazaga, A.; Lio, P.; and Micklem, G. 2024. HyperBERT: Mixing Hypergraph-Aware Layers with Language Models for Node Classification on Text-Attributed Hypergraphs. In *Findings of the Association for Computational Linguistics: EMNLP 2024*.

Bron, C.; and Kerbosch, J. 1973. Algorithm 457: finding all cliques of an undirected graph. *Commun. ACM*.

Chien, E.; Chang, W.-C.; Hsieh, C.-J.; Yu, H.-F.; Zhang, J.; Milenkovic, O.; and Dhillon, I. S. 2022a. Node feature extraction by self-supervised multi-scale neighborhood prediction. In *International Conference on Learning Representations (ICLR)*.

Chien, E.; Pan, C.; Peng, J.; and Milenkovic, O. 2022b. You are AllSet: A Multiset Function Framework for Hypergraph Neural Networks. In *International Conference on Learning Representations (ICLR)*.

Devlin, J.; Chang, M.-W.; Lee, K.; and Toutanova, K. 2019. Bert: Pre-training of deep bidirectional transformers for language understanding. In *Proceedings of the 2019 conference of the North American chapter of the association for computational linguistics: human language technologies, volume 1 (long and short papers)*, 4171–4186.

Fang, X.; Wang, B.; Huan, C.; Ma, S.; Zhang, H.; and Zhao, C. 2025. HyperKAN: Hypergraph Representation Learning with Kolmogorov-Arnold Networks. *arXiv preprint arXiv:2503.12365*.

Fang, Y.; Fan, D.; Zha, D.; and Tan, Q. 2024. Gaugllm: Improving graph contrastive learning for text-attributed graphs with large language models. In *Proceedings of the 30th ACM SIGKDD Conference on Knowledge Discovery and Data Mining*, 747–758.

Feng, Y.; You, H.; Zhang, Z.; Ji, R.; and Gao, Y. 2019. Hypergraph neural networks. In *Proceedings of the AAAI conference on artificial intelligence*, 3558–3565.

Giles, C. L.; Bollacker, K. D.; and Lawrence, S. 1998. CiteSeer: an automatic citation indexing system. In *Proceedings of the Third ACM Conference on Digital Libraries*, 89–98. New York, NY, USA: Association for Computing Machinery.

He, P.; Liu, X.; Gao, J.; and Chen, W. 2020. Deberta: Decoding-enhanced bert with disentangled attention. *arXiv preprint arXiv:2006.03654*.

He, X.; Bresson, X.; Laurent, T.; Perold, A.; LeCun, Y.; and Hooi, B. 2024. Harnessing explanations: Llm-to-lm interpreter for enhanced text-attributed graph representation learning. In *International Conference on Learning Representations (ICLR)*.

Hou, Z.; Liu, X.; Cen, Y.; Dong, Y.; Yang, H.; Wang, C.; and Tang, J. 2022. Graphmae: Self-supervised masked graph autoencoders. In *Proceedings of the 28th ACM SIGKDD conference on knowledge discovery and data mining*, 594–604.

Hu, E. J.; Shen, Y.; Wallis, P.; Allen-Zhu, Z.; Li, Y.; Wang, S.; Wang, L.; Chen, W.; et al. 2022. Lora: Low-rank adaptation of large language models. *ICLR*, 1(2): 3.

Kim, S.; Bu, F.; Choe, M.; Yoo, J.; and Shin, K. 2023. How transitive are real-world group interactions?-measurement and reproduction. In *Proceedings of the 29th ACM SIGKDD Conference on Knowledge Discovery and Data Mining*, 1132–1143.

Kim, S.; Kang, S.; Bu, F.; Lee, S. Y.; Yoo, J.; and Shin, K. 2024a. Hypeboy: Generative self-supervised representation learning on hypergraphs. In *International Conference on Learning Representations (ICLR)*.

Kim, S.; Lee, S. Y.; Gao, Y.; Antelmi, A.; Polato, M.; and Shin, K. 2024b. A survey on hypergraph neural networks: an in-depth and step-by-step guide. In *Proceedings of the 30th ACM SIGKDD Conference on Knowledge Discovery and Data Mining*, 6534–6544.

Lee, D.; and Shin, K. 2023. I'm me, we're us, and i'm us: Tri-directional contrastive learning on hypergraphs. In *Proceedings of the AAAI conference on artificial intelligence*, 8456–8464.

Lee, G.; Lee, S. Y.; and Shin, K. 2024. VilLain: Self-Supervised Learning on Homogeneous Hypergraphs without Features via Virtual Label Propagation. In *Proceedings of the ACM Web Conference 2024, WWW '24*, 594–605.

Li, F.; Wang, X.; Cheng, D.; Zhang, W.; Zhang, Y.; and Lin, X. 2024. Hypergraph self-supervised learning with sampling-efficient signals. In *Proceedings of the Thirty-Third International Joint Conference on Artificial Intelligence, IJCAI '24*.

Liu, Y.; Ott, M.; Goyal, N.; Du, J.; Joshi, M.; Chen, D.; Levy, O.; Lewis, M.; Zettlemoyer, L.; and Stoyanov, V. 2019. Roberta: A robustly optimized bert pretraining approach. *arXiv preprint arXiv:1907.11692*.

Mikolov, T.; Sutskever, I.; Chen, K.; Corrado, G. S.; and Dean, J. 2013. Distributed representations of words and phrases and their compositionality. *Advances in neural information processing systems*, 26.

Ni, J.; Li, J.; and McAuley, J. 2019. Justifying Recommendations using Distantly-Labeled Reviews and Fine-Grained Aspects. In *Proceedings of the 2019 Conference on Empirical Methods in Natural Language Processing and the 9th International Joint Conference on Natural Language Processing (EMNLP-IJCNLP)*.

Oord, A. v. d.; Li, Y.; and Vinyals, O. 2018. Representation learning with contrastive predictive coding. *arXiv preprint arXiv:1807.03748*.

Preti, G.; De Francisci Morales, G.; and Bonchi, F. 2024. Hyper-distance oracles in hypergraphs. *The VLDB Journal*, 33(5): 1333–1356.

Sanh, V.; Debut, L.; Chaumond, J.; and Wolf, T. 2019. DistilBERT, a distilled version of BERT: smaller, faster, cheaper and lighter. *arXiv preprint arXiv:1910.01108*.

Schroff, F.; Kalenichenko, D.; and Philbin, J. 2015. Facenet: A unified embedding for face recognition and clustering. In *Proceedings of the IEEE conference on computer vision and pattern recognition*.

Sen, P.; Namata, G.; Bilgic, M.; Getoor, L.; Gallagher, B.; and Eliassi-Rad, T. 2008. Collective Classification in Network Data Articles. *AI Magazine*, 29: 93–106.

Thakoor, S.; Tallec, C.; Azar, M. G.; Azabou, M.; Dyer, E. L.; Munos, R.; Veličković, P.; and Valko, M. 2022. Large-scale representation learning on graphs via bootstrapping. In *International Conference on Learning Representations (ICLR)*.

Wang, Y.; and Kleinberg, J. 2024. From graphs to hypergraphs: Hypergraph projection and its remediation. *arXiv preprint arXiv:2401.08519*.

Wang, Y.; Zhu, Y.; Zhang, W.; Zhuang, Y.; Liyunfei, L.; and Tang, S. 2024. Bridging Local Details and Global Context in Text-Attributed Graphs. In *Proceedings of the 2024 Conference on Empirical Methods in Natural Language Processing*.

Wei, T.; You, Y.; Chen, T.; Shen, Y.; He, J.; and Wang, Z. 2022. Augmentations in hypergraph contrastive learning: Fabricated and generative. *Advances in neural information processing systems*, 35: 1909–1922.

Wu, Y.; Wang, L.; Han, X.; and Ye, H.-J. 2024. Graph contrastive learning with cohesive subgraph awareness. In *Proceedings of the ACM Web Conference 2024*, 629–640.

Xia, L.; Huang, C.; and Zhang, C. 2022. Self-supervised hypergraph transformer for recommender systems. In *Proceedings of the 28th ACM SIGKDD conference on knowledge discovery and data mining*, 2100–2109.

Yan, H.; Li, C.; Long, R.; Yan, C.; Zhao, J.; Zhuang, W.; Yin, J.; Zhang, P.; Han, W.; Sun, H.; et al. 2023. A comprehensive study on text-attributed graphs: Benchmarking and rethinking. *Advances in Neural Information Processing Systems*, 36: 17238–17264.

Yang, J.; Liu, Z.; Xiao, S.; Li, C.; Lian, D.; Agrawal, S.; Singh, A.; Sun, G.; and Xie, X. 2021. Graphformers: Gnn-nested transformers for representation learning on textual graph. *Advances in Neural Information Processing Systems*, 34: 28798–28810.

You, Y.; Chen, T.; Sui, Y.; Chen, T.; Wang, Z.; and Shen, Y. 2020. Graph contrastive learning with augmentations. *Advances in neural information processing systems*, 33: 5812–5823.

Yu, S.; Yang, H.; Nakahara, H.; Santos, G. S.; Nikolić, D.; and Plenz, D. 2011. Higher-order interactions characterized in cortical activity. *Journal of neuroscience*, 31(48): 17514–17526.

Yu, S. K.; Lee, D. E.; Ko, Y.; and Kim, S.-W. 2025. HyGEN: Regularizing Negative Hyperedge Generation for Accurate Hyperedge Prediction. In *Companion Proceedings of the ACM on Web Conference 2025*, 1500–1504.

Zhang, P.; Li, C.; Kang, L.; Huang, F.; Wang, S.; Xie, X.; and Kim, S. 2024. High-frequency-aware hierarchical contrastive selective coding for representation learning on text attributed graphs. In *Proceedings of the ACM Web Conference 2024*, 4316–4327.

Zhang, Y.; Jin, R.; and Zhou, Z.-H. 2010. Understanding bag-of-words model: a statistical framework. *International Journal of Machine Learning and Cybernetics*, 1: 43–52.

Zhao, J.; Qu, M.; Li, C.; Yan, H.; Liu, Q.; Li, R.; Xie, X.; and Tang, J. 2023. Learning on large-scale text-attributed graphs via variational inference. In *International Conference on Learning Representations (ICLR)*.

Appendix

A Additional Experimental Setup

A.1 Datasets

Since no publicly available benchmark datasets are specifically designed for Text-Attributed Hypergraphs (TAHGs), we construct six datasets spanning two domains: academic co-citation networks and E-commerce platforms. Basic statistics are summarized in Table 1.

Co-citation hypergraphs. We construct two academic hypergraphs, Citeseer (Giles, Bollacker, and Lawrence 1998) and Cora (Sen et al. 2008), based on the standard citation networks, where each node represents a scientific publication. The textual attributes of each node, including the title and abstract, are directly adopted from prior works (He et al. 2024; Wang et al. 2024). To capture high-order relationships, we define a hyperedge as the set of all papers that co-cite the same reference.

E-commerce hypergraphs. We further construct four e-commerce hypergraphs from the Amazon product network (Ni, Li, and McAuley 2019): Book-History, Ele-Photo, Ele-Computers, and Sports-Fitness. In these datasets, each node represents a product, and edges reflect frequent co-purchase or co-browsing behavior. The raw textual attributes of nodes are obtained from the annotations provided by (Yan et al. 2023). Specifically, in Book-History, textual features include book titles and descriptions; in Ele-Computers and Ele-Photo, they consist of high-rated reviews and product summaries; in Sports-Fitness, only product titles are used. To induce high-order structures, we adopt a max-clique-based reconstruction strategy (Bron and Kerbosch 1973; Wang and Kleinberg 2024), where hyperedges are formed by identifying maximal cliques in the co-purchase graph.

A.2 Baselines

We compare our method against seven strong self-supervised learning (SSL) baselines, covering both graph-based and hypergraph-based paradigms.

Graph-based SSL. In this work, we adopt three widely used graph-based SSL frameworks: two contrastive learning methods, GraphCL (You et al. 2020) and BGRL (Thakoor et al. 2022), and one generative method, GraphMAE (Hou et al. 2022). To adapt these methods to hypergraphs, we apply clique expansion following the protocol in (Lee and Shin 2023). For textual feature extraction, we employ shallow encoders (SE) implemented via Skip-Gram (Mikolov et al. 2013), as well as GIANT (Chien et al. 2022a), a graph-agnostic text encoder designed for raw textual attributes.

Hypergraph-based SSL. We include four state-of-the-art hypergraph SSL methods: two contrastive approaches, TriCL (Lee and Shin 2023) and SE-HSSL (Li et al. 2024); one generative method, HypeBoy (Kim et al. 2024a); and VilLain (Lee, Lee, and Shin 2024), which targets the feature-absent setting. All methods adopt the same SE setup and are additionally evaluated with two pre-trained language models: BERT-Base (Devlin et al. 2019) and RoBERTa-Base (Liu et al. 2019).

A.3 Evaluation Protocol

We evaluate our method on two standard hypergraph learning tasks: node classification and hyperedge prediction. After pretraining with HiTeC, we adopt a linear evaluation protocol (Lee and Shin 2023; Li et al. 2024; Kim et al. 2024a), where the pretrained node embeddings are frozen and used as input features for downstream classifiers.

Node classification. Following (Lee and Shin 2023; Li et al. 2024), we randomly split each dataset into 10%/10%/80% for training, validation, and testing. Then, a simple linear classifier is trained on top of the fixed node embeddings using ℓ_2 -regularized logistic regression. We report the average test accuracy and standard deviation over 20 random splits, each with 5 different initializations.

Hyperedge prediction. Following (Kim et al. 2024a), we need to generate negative hyperedge samples to evaluate a model on the hyperedge prediction task. In our experiments, we adopt Clique Negative Sampling (CNS) (Yu et al. 2025), a widely used strategy for constructing negative hyperedge samples. Specifically, for a given hyperedge e , we replace a node $u \in e$ with a node $v \notin e$ such that v is connected to all other nodes in e , i.e., $(e \setminus \{u\}) \cup \{v\}$. Then, a two-layer MLP is trained on the fixed node embeddings using the 60%/20%/20% data split. Same as the node classification task, we report the average test accuracy and standard deviation over 20 random splits, each with 5 initializations.

A.4 Implementation Details

All experiments are conducted on a single NVIDIA A5000 GPU (24GB memory). For all baselines, we adopt their official implementations with default settings. For HiTeC, we adopt BERT-Base (Devlin et al. 2019) as the text encoder and apply LoRA (Hu et al. 2022) for parameter-efficient fine-tuning. The text encoder is trained for 5 epochs on small datasets (Citeseer, Cora), 4 epochs on medium datasets (History, Photo), and 3 epochs on large datasets (Computers, Fitness), using a learning rate of 2e-5. The hypergraph encoder is implemented as a single-layer module. We tune the contrastive loss weight λ_e and λ_s over $\{1, 2, 3, 4\}$. The overlap threshold s and subgraph sampling ratio $r\%$ are tuned from $\{1, 2, 3, 4, 5, 10\}$ and $\{10\%, 20\%, 30\%, 40\%, 50\%\}$, respectively. To ensure a fair comparison, we tune the learning rate from $\{0.01, 0.001, 1e-4, 5e-4\}$ and weight decay from $\{0, 1e-5\}$ for all methods.

B Additional Experiment Results

B.1 Hyperedge Prediction Evaluation

We further evaluate all models on the hyperedge prediction task, with results presented in Table 3. The key observations are as follows: (1) Graph-based SSL methods remain less effective. Their performance is still hindered by the loss of high-order structure due to clique expansion. Although GIANT achieves slight improvements, probably due to its pseudo-labeling strategy for edge-level supervision, it still underperforms compared to HSSL methods enhanced with pre-trained language models. (2) HiTeC achieves the best performance on 5 out of 6 datasets, demonstrating strong

Method	Citeseer	Cora	History	Photo	Computers	Fitness
Graph SSL	GraphCL + SE	69.48 ± 2.07	59.05 ± 2.16	65.65 ± 1.06	67.48 ± 1.18	68.66 ± 1.33
	GraphCL + GIANT	72.70 ± 2.06	55.48 ± 1.96	63.02 ± 1.61	68.78 ± 1.16	70.87 ± 0.87
	BGRL+SE	70.08 ± 2.38	62.45 ± 2.48	64.47 ± 1.18	64.76 ± 1.23	64.66 ± 1.40
	BGRL + GIANT	72.61 ± 1.99	66.22 ± 2.38	65.13 ± 2.09	65.65 ± 1.10	67.67 ± 0.99
	GraphMAE + SE	71.71 ± 1.78	64.85 ± 1.66	59.81 ± 0.27	66.33 ± 1.58	64.83 ± 1.72
	GraphMAE + GIANT	72.25 ± 1.62	66.30 ± 2.19	64.19 ± 0.23	64.83 ± 0.20	66.10 ± 1.20
HSSL	TriCL + SE	68.06 ± 1.75	62.43 ± 2.41	67.18 ± 0.24	69.21 ± 0.19	70.63 ± 0.14
	TriCL + BERT	71.36 ± 1.78	64.02 ± 2.33	70.18 ± 0.31	71.71 ± 0.21	73.20 ± 0.17
	TriCL + RoBERTa	72.38 ± 1.37	66.49 ± 1.93	68.34 ± 0.58	70.35 ± 0.28	72.20 ± 0.27
	SE-HSSL + SE	64.80 ± 2.21	65.57 ± 1.88	63.49 ± 1.98	65.42 ± 0.74	66.44 ± 1.09
	SE-HSSL + BERT	72.29 ± 1.74	65.66 ± 2.25	67.93 ± 0.44	71.27 ± 0.18	70.68 ± 0.91
	SE-HSSL + RoBERTa	73.09 ± 1.56	65.86 ± 1.94	66.95 ± 0.53	69.65 ± 0.20	71.19 ± 0.16
	HypeBoy + SE	71.93 ± 2.04	65.17 ± 1.66	OOM	OOM	OOM
	HypeBoy + BERT	74.56 ± 2.10	67.38 ± 1.89	OOM	OOM	OOM
	HypeBoy + RoBERTa	73.47 ± 2.10	66.51 ± 1.87	OOM	OOM	OOM
	VilLain (w/o feat.)	74.25 ± 1.90	63.25 ± 2.57	63.18 ± 0.35	65.02 ± 0.23	65.85 ± 0.28
HiTeC	HyperBERT	51.84 ± 2.03	45.32 ± 1.47	OOM	OOM	OOM
		74.60 ± 1.84	65.91 ± 2.32	71.83 ± 0.21	72.56 ± 0.17	73.91 ± 0.14
						67.32 ± 0.09

Table 3: Evaluation results on hyperedge prediction (% mean \pm std). The **best** and second-best results are highlighted in **bold** and underline, respectively. ‘w/o feat.’ means without node features. OOM denotes out-of-memory on a 24GB GPU.

Dataset	DistilBERT	BERT	RoBERTa	DeBERTa
Citeseer	67.54 ± 1.49	66.38 ± 1.73	65.09 ± 1.26	64.83 ± 4.65
Cora	74.55 ± 0.02	74.07 ± 0.88	72.32 ± 0.91	70.41 ± 2.24
History	78.05 ± 0.18	<u>79.81 ± 0.16</u>	74.77 ± 0.24	76.20 ± 0.12
Photo	56.90 ± 0.31	<u>59.64 ± 0.16</u>	54.15 ± 0.40	52.54 ± 0.08
Computers	50.64 ± 0.25	<u>55.81 ± 0.12</u>	52.36 ± 0.21	51.48 ± 0.56
Fitness	62.97 ± 0.08	<u>67.18 ± 0.19</u>	64.98 ± 0.78	65.29 ± 0.14

Table 4: Different text encoder backbones.

generalizability between tasks. TriCL and SE-HSSL underperform due to their limited capacity to capture long-range dependencies. HypeBoy exhibits competitive results on small-scale hypergraphs, benefiting from its hyperedge-filling strategy, but fails to scale to larger datasets, indicating poor scalability. Overall, HiTeC exceeds the second-best method by 1.65% and 1.15% on History and Fitness, respectively, demonstrating its robustness and scalability across diverse hypergraph scenarios.

B.2 Impact of Text Encoder Backbones

We conduct an ablation study on different text encoder backbones, including DistilBERT (Sanh et al. 2019), BERT-Base (Devlin et al. 2019), RoBERTa-Base (Liu et al. 2019), and DeBERTa-Base (He et al. 2020), as shown in Table 4. Among these, BERT achieves the highest overall performance, followed by DistilBERT. These results suggest that selecting a suitable text encoder for each dataset is important. Nevertheless, our framework is compatible with various backbones. In our main experiments, we adopt BERT as the default text encoder backbone.

B.3 Parameter Sensitivity Analysis of Subgraph Sampling Ratio $r\%$

We further perform a sensitivity analysis by varying the subgraph sampling ratio $r\% \in \{10\%, 20\%, 30\%, 40\%, 50\%\}$.

As shown in Figure 7, model performance generally increases rapidly at first and then plateaus, while training time grows sharply with larger r . Notably, on most datasets, setting $r\% = 30\%$ achieves comparable accuracy to $r\% = 50\%$, while significantly reducing training time. For example, on Computers and Fitness, $r\% = 30\%$ leads to $2.4\times$ and $2.6\times$ speedups, respectively, with only marginal drops in accuracy. These results indicate that selecting a small number of structurally central nodes based on degree ranking enables efficient subgraph-level representation learning without sacrificing performance. In our main experiments, we report the results with $r\% = 30\%$, which achieves a trade-off between efficiency and performance.

C Additional Related Work

C.1 Representation Learning on TAGs

Since hypergraphs can be transformed into graphs via clique expansion, our work is closely related to representation learning on text-attributed graphs (TAGs). Recent TAG methods leverage pre-trained language models to generate numerical features, typically in a cascade (He et al. 2024; Wang et al. 2024) or nested (Yang et al. 2021; Zhao et al. 2023) manner. While most existing TAG methods are supervised, emerging efforts explore self-supervised learning (SSL) to reduce annotation costs. GIANT (Chien et al. 2022a) makes an early attempt by aligning textual and structural features via an extreme multi-label classification objective. More recently, GAugLLM (Fang et al. 2024) proposes an augmentation framework that utilizes large language models (LLMs) to perturb both node features and graph structure, while HASH-CODE (Zhang et al. 2024) formulates a multi-objective contrastive learning strategy tailored for TAGs. However, adapting these methods to hypergraphs via clique expansion incurs substantial structural loss, limiting their effectiveness on TAHGs and motivating the need for dedicated HSSL approaches.

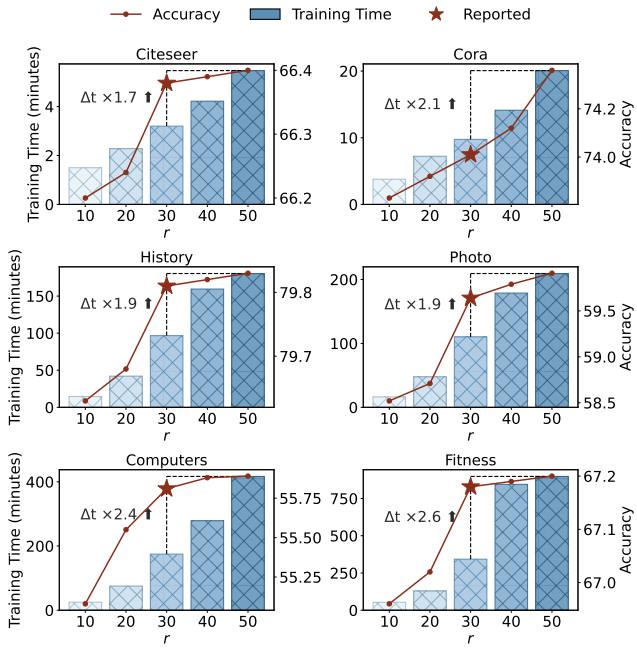


Figure 7: Training time and accuracy under different sampling ratios $r\%$. Bar plots represent training time (in minutes), while line plots indicate the corresponding accuracy. We highlight the relative speedup Δt of $r\% = 30\%$ over $r\% = 50\%$. All main results are reported with $r\% = 30\%$.